Journal of Hazardous Materials 219–220 (2012) 148–155

Contents lists available at SciVerse ScienceDirect

Journal of Hazardous Materials

journal homepage: www.elsevier.com/locate/jhazmat

Toxic effect of different ZnO particles on mouse alveolar macrophages

Jinyang Zhang[a,d], Wenhua Song[a,b,*], Jing Guo[b], Jinhua Zhang[b], Zengtian Sun[b], Feng Ding[c], Minling Gao[b]

[a] College of Environmental Science and Engineering, Shanghai Jiaotong University, Shanghai 200240, China
[b] School of Environmental and Chemical Engineering, Tianjin Polytechnic University, Tianjin 300160, China
[c] College of Environmental Science and Engineering, Nankai University, Tianjin 300071, China
[d] College of Chemical and Environmental Engineering, Neijiang Normal University, Neijiang, 641112, China

ARTICLE INFO

Article history:
Received 12 December 2011
Received in revised form 21 February 2012
Accepted 26 March 2012
Available online 3 April 2012

Keywords:
ZnO nanoparticles
Mouse alveolar macrophages
Toxic effect
Cell apoptosis
Antioxidation
Synthesis

ABSTRACT

To study the toxicity mechanism of ZnO nanoparticles on mouse macrophages, the toxic effect of different ZnO nanoparticles on mouse alveolar macrophages (MH-S) was investigated in this study. The results showed that the 24 h IC_{50} of four ZnO particles were 48.53, 47.37, 45.43 and 26.74 μg/ml for bulk ZnO, 100 nm, 30 nm and 10–30 nm ZnO particles, respectively. At the concentration of 10 μg/ml and below, dissolved zinc ions induced metallothionein synthesis, enhanced cellular resistance to oxidative stress. ZnO particles mainly induced cell apoptosis. When the concentration of ZnO particles was 20 μg/ml and above, excessive zinc destroyed mitochondrial function and cell membrane, caused cell necrosis. Dissolved zinc ions first cause toxicity in MH-S cells. However, the toxic effect of dissolved zinc ions may exist a threshold on mouse macrophages, inducing about 50% cell death. The toxic difference of different ZnO particles mainly depended on the effect of nondissolved ZnO particles.

1. Introduction

In recent years, health hazards of nanoparticles have been a research focus. Many studies in vitro demonstrated that ZnO nanoparticles are toxic to mammalian cells, even more toxic than other nanometer-scale structures metallic oxide [1–3]. Brunner et al. showed that a three-day exposure of human mesothelioma and rodent fibroblast cell to 15 μg/ml ZnO nanoparticles (19 nm) caused DNA and mitochondrial damage [4]. Karlsson et al. found that ZnO nanoparticles (71 nm) decreased cell viability and caused oxidative DNA damage in human alveolar epithelial cell (A549) at the concentration above 40 μg/ml [5]. Xia et al. found that ZnO nanoparticles induced toxicity in RAW264.7 and BEAS-2B cells, leading to the generation of reactive oxygen species (ROS), oxidant injury, and cell death [6]. Lin et al. reported that exposure of A549 cells to ZnO nanoparticles (70–420 nm) at the dose above 10 μg/ml induced increases in oxidative stress, lipid peroxidation, cell membrane disruption, and DNA damage [7]. Kim et al. investigated ZnO nanoparticles-induced injury to alveolar epithelium by exposing primary cultured rat alveolar epithelial cell monolayers (RAECMs) to ZnO nanoparticles. Researchers found that exposure to ZnO nanoparticles induced severe injury in RAECMs and destroyed cell membrane integrity at the dose above 22 μg/ml, and Zn^{2+} derived from ZnO nanoparticles, mitochondrial dysfunction and increased level of intracellular ROS played important roles in ZnO nanoparticles-induced injury in RAECMs [8]. Our previous study also found ZnO nanoparticles reduced cell viability in mouse peritoneal macrophage (Ana-1), induced lactate dehydrogenase (LDH) leakage and increased level of intracellular ROS. The dissolved Zn^{2+} played a main role in toxic effect of ZnO particles [9]. In addition, Baird et al. reported Zn-mediated metallothionein (MT) up-regulation protected against oxidative stress-induced cellular injury [10]. However, at present, there are few reports on the effect of ZnO nanoparticles on MT in cell.

Alveolar macrophage (AM) is an important cell to protect lung. It is the first line of defense of the respiratory tract. To some extent, the activity of alveolar macrophage could be used as an important indicator of response evaluation of the lungs [11]. Beyerle et al. showed that 70 nm ZnO naoparticles were more toxic in MH-S cells than in LA4 cells [12]. In order to further study toxicity mechanism of ZnO particles on mouse macrophage, we took mouse alveolar macrophages (MH-S cells) as the subject, investigated the effects

* Corresponding author at: School of Environmental and Chemical Engineering, Tianjin Polytechnic University, Tianjin 300160, China. Tel.: +086 022 83956732; fax: +086 022 83956667.
E-mail address: songwenhua9316@sina.com (W. Song).

0304-3894/$ – see front matter © 2012 Elsevier B.V. All rights reserved.
http://dx.doi.org/10.1016/j.jhazmat.2012.03.069

Table 1
Characterization of ZnO particles.

ZnO	Size and distribution (nm)	SSA (m^2/g)	Crystalline structure	Shape
Bulk ZnO	Length: 341.75 ± 173.34 Diameter: 173.48 ± 72.73	2.52	Hexagonal	Rod
100 nm	Length: 107.59 ± 38.44 Diameter: 60.21 ± 21.76	8.67	Hexagonal	Rod
30 nm	Length: 70.89 ± 34.18 Diameter: 40.44 ± 12.51	9.24	Hexagonal	Rod
10–30 nm	18.76 ± 4.98	41.71	Hexagonal	Sphericity

of different ZnO nanoparticles on cell viability, LDH leakage, cell apoptosis, oxidative stress, mitochondrial function and MT expression, and compared with the cytotoxicity of ZnO particles in Ana-1 cells in this study.

2. Materials and methods

2.1. ZnO particles

Four types of ZnO particles were purchased from different commercial companies. Bulk ZnO particles (<1 μm) were purchased from Hangzhou Wanjingxin Material Co. Ltd., China. 100 ± 10 nm and 30 ± 10 nm ZnO nanoparticles were purchased from Beijing Nachen Technology Co. Ltd., China. 10–30 nm ZnO nanoparticles were purchased from Shenzhen Nanuo Nanomaterials Corp. Visualize particles size and shape of ZnO particles was measured by transmission electron microscopy (TEM) (H7650). Crystal structure of ZnO particles was characterized using X-ray diffraction (XRD) (Bruker D8 Discover) [9]. Particle specific surface area (SSA) was determined by BET surface area analyzer (AUTOSORB-MP). The characterization data were shown in Table 1.

2.2. Cell culture and treatment with ZnO particles

Mouse alveolar macrophage cell line was purchased from American Type Culture Collection (ATCC). Cells were cultured at 37 °C with 5% CO_2 in the complete cell medium, RPMI1640 media supplemented with 10% fetal bovine serum (FBS), 100 U/ml penicillin, 100 μg/ml streptomycin and 2 mM L-glutamine.

1 mg/ml ZnO nanoparticles suspensions were prepared with the complete cell medium to yield a more accurate weighing of ZnO powder, dispersed for 20 min by a sonicator to prevent aggregation, and diluted to the specified concentrations (2.5, 5, 10, 20, 40, 80, 100 μg/ml) for treatment of cells.

The preparation process of the supernatants of ZnO nanoparticles was as following: 2.5, 5.0, 10.0, 20.0, 40.0, 80.0 or 100.0 μg/ml of ZnO nanoparticles suspensions were incubated at 37 °C in a humidified 5% CO_2 environment for 24 h, centrifuged at 20,000 rpm for 30 min and collected the supernatants.

2.3. Cell viability assay

Cellular viability was determined using the CCK-8 assay (Beyotime). Cells were seeded with equal density in each well of 96-well plates (10^4 cells per well), 100 μl of the cell culture medium per well, and incubated for 24 h at 37 °C. Then cells were treated in 96-well plates with 2.5, 5.0, 10.0, 20.0, 40.0, 80.0 or 100.0 μg/ml of ZnO particles for 24 h at 37 °C. Untreated cells served as a control group. At the end of the treatment, CCK-8 dye was added to each well and the plates were incubated for another 2 h at 37 °C. To prevent particles from interfering with this assay, the solution in each well of each plate was quantitatively transferred to an empty well in another plate. Subsequently, the absorbance was measured by dual wavelength spectrophotometry at 450 nm and 630 nm using a microplate reader. Each treatment was repeated five times.

In order to investigate the effect of zinc ions released from ZnO particles on cell viability, the supernatants of ZnO particles suspensions were used to treat cells, and the cell viability was assayed by CCK-8.

2.4. LDH measurement

Release of lactate dehydrogenase (LDH) to the cell culture medium indicates cell membrane damage. LDH level in the cell culture medium was determined using a LDH Kit (Jiancheng Bioengineering Co. Ltd, Nanjing, China) according to the manufacturer's protocols. LDH catalyzed the oxidation of lactate to pyruvate with simultaneous reduction of NAD^+ to NADH. The rate of NAD^+ reduction is directly proportional to LDH level. Cells were seeded with equal density in each well of 96-well plates (10^4 cells per well), 200 μl of the cell culture medium per well, and incubated for 24 h at 37 °C. After ZnO nanoparticles suspensions and their supernatants exposure, half the amount of the 200 μl cell culture medium was collected for LDH analysis. Absorption was measured at 340 nm.

2.5. Apoptosis and necrosis of MH-S cells

Apoptosis and necrosis of MH-S cells was assayed by double staining with Annexin V-R-PE and 7-AAD by flow cytometer (BD Biosciences, USA). After treatment with 5, 10, 20, 40 and 80 μg/ml ZnO particles for 24 h, MH-S cells were collected, washed twice with cold PBS, and resuspended to 10^6 cells/ml in 200 μl binding buffer. 100 μl of MH-S cells was transferred to a 1.5 ml culture tube, added to by 10 μl of Annexin V-R-PE, incubated at 4 °C in the dark for 30 min, and then added 10 μl of 7-AAD in the dark. Stained MH-S cells were analyzed by the flow cytometer.

2.6. Intracellular reactive oxygen species measurement

The intracellular ROS was determined using a well-characterized probe, 2′, 7′-dichlorofluorescein diacetate (DCFH-DA) (Beyotime, China) [13]. DCFH-DA passively enters the cell, and is hydrolyzed by esterases to DCFH. This nonfluorescent molecule is then oxidized to fluorescent compound dichlorofluorescein (DCF) by cellular oxidants. A DCFH-DA stock solution (in methanol) of 10 mM was diluted 1000-fold in the cell

culture medium without serum or other additives to yield a 10 μM working solution. Cells were seeded with equal density in each well of 6-well plates (4×10^5 cells per well), 2 ml of the cell culture medium per well, and incubated for 24 h at 37 °C. Then cells were treated with 2.5, 5.0, 10.0, 20.0, 40.0, 80.0 or 100.0 μg/ml of ZnO nanoparticles for 24 h at 37 °C. Cells were washed twice with PBS and then incubated with DCFH-DA working solution for 20 min in the dark environment (37°Cincubator) followed by treatment with ZnO nanoparticles for 24 h. Then the cells were washed three times with cell culture medium without serum to eliminate DCFH-DA that did not enter the cells. Cells were collected in suspension. The fluorescence was determined at 488 nm excitation and 525 nm emission using a fluorospectrophotometer.

2.7. Intracellular calcium concentrations measurement

Fluo-3-AM (Beyotime, China) was used to measure intracellular calcium concentrations. Cells were seeded with equal density in each well of 6-well plates (4×10^5 cells per well), 2 ml of the cell culture medium per well, and incubated for 24 h at 37 °C. Then cells were treated with 2.5, 5.0, 10.0, 20.0, 40.0, 80.0 or 100.0 μg/ml of ZnO nanoparticles for 24 h at 37 °C. The culture medium was discarded, and the cells were washed two times with PBS buffer and then incubated with Fluo-3-AM working solution for 30 min in the dark environment (37°Cincubator). The cells were collected by centrifuging at 600 g for 5 min and washing two times with PBS buffer. And then the cells were resuspended with PBS buffer. The fluorescence was determined at 488 nm excitation and 525 nm emission using a fluorospectrophotometer.

2.8. Mitochondrial membrane potential detection

The fluorescent, lipophilic and cationic probe, JC-1 (Beyotime, China), was used to determine the mitochondrial membrane potential ($\Delta\psi m$) of MH-S cells according to the manufacturer's directions. Briefly, cells were seeded with equal density in each well of 6-well plates (4×10^5 cells per well), 2 ml of the cell culture medium per well, and incubated for 24 h at 37 °C. Then cells were treated with 2.5, 5.0, 10.0, 20.0, 40.0, 80.0 or 100.0 μg/ml ZnO nanoparticles. After exposure to ZnO nanoparticles for 24 h, the cells were incubated with JC-1 staining solution for 20 min at 37 °C, and then rinsed twice with JC-1 staining buffer. The fluorescence intensity of both mitochondrial JC-1 monomers (λ ex 490 nm, λ em 530 nm) and aggregates (λ ex 525 nm, λ em 590 nm) were detected using a fluorospectrophotometer. The $\Delta\psi m$ of MH-S cells were calculated as the fluorescence ratio of red (i.e. aggregates) to green (i.e. monomers).

2.9. MT assay

Cells were seeded with equal density in each well of 6-well plates (4×10^5 cells per well), 2 ml of the cell culture medium per well, and incubated for 24 h at 37 °C. MH-S cells were collected followed by treatment with ZnO nanoparticles for 24 h, and were lysed using ultrasonic wave. The cell lysates were then centrifuged at 10,000 rpm for 10 min at 4 °C. MT content was assayed by ELISA kit (BlueGene) according to the manufacturer's instructions.

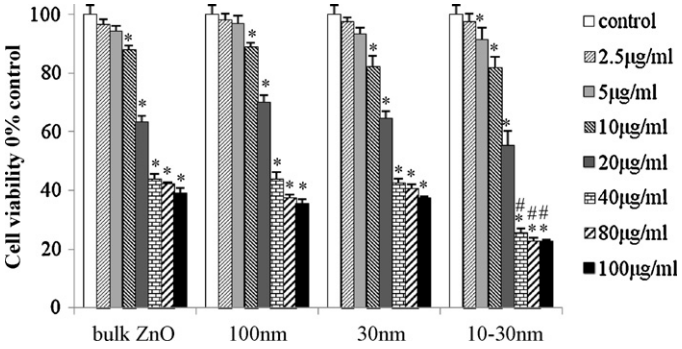

Fig. 1. Cell viability of MH-S cell exposed to different ZnO particles for 24 h. Each treatment was conducted five times independently. * $p < 0.05$ vs. control cells; # $p < 0.05$ vs. other sized ZnO nanoparticles.

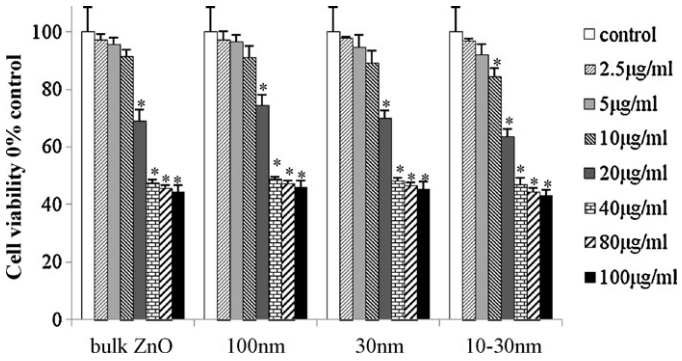

Fig. 2. Cell viability of MH-S cell exposed to supernatants of ZnO particles suspensions incubated for 24 h. Each treatment was conducted five times independently. * $p < 0.05$ vs. control cells.

2.10. Statistical analysis

The data were expressed as mean ±standard deviation. For statistical analysis, the experimental values were compared to their corresponding control values. A one-way analysis of variance (ANOVA) in SPSS software (Version 16.0) was used to illustrate the significant difference between the experimental group and the control. The significant difference was considered to be $p < 0.05$.

3. Results and discussion

3.1. Cytotoxicity of ZnO particles in MH-S cells

Fig. 1 showed cell viability of MH-S cells after exposed to ZnO particles. The 24 h IC_{50} values of four ZnO particles were 48.53, 47.37, 45.43 and 26.74 μg/ml for bulk ZnO, 100 nm, 30 nm and 10–30 nm ZnO particles, respectively (Table 2). When ZnO particles concentrations exceeded 40 μg/ml, 10–30 nm ZnO particles induced lower cell viability than other ZnO particles. Fig. 2 showed the effect of supernatants of ZnO particles suspensions on cell viability. When the concentration of ZnO particles exceeded 20 μg/ml, the supernatants of ZnO particles suspensions reduced cell viability markedly ($p < 0.05$). When the concentrations of ZnO particles exceeded 40 μg/ml, the supernatants of ZnO particles suspensions

Table 2
The 24 h IC_{50} values and 95% confidence limits for MH-S cells exposed different ZnO particles.

	ZnO			
	Bulk ZnO	100 nm	30 nm	10–30 nm
ZnO concentration (μg/ml)	48.53	47.37	45.43	26.74
95% confidence limits	42.00–57.00	42.17–53.69	39.80–52.49	23.61–30.32

all decreased cell viability to 50–55%, and cell viability had little change with the increase of ZnO particles concentrations.

In our previous study, we investigated the cytotoxicity of ZnO particles in Ana-1 cells [9]. 24 h IC_{50} values of ZnO particles in Ana-1 cells were 30.95, 40.41, 43.94 and 44.56 μg/ml for 10–30 nm, 30 nm, 100 nm and bulk ZnO particles, respectively. The dissolved zinc ions induced about 50% cell death. Therefore, ZnO particles had similar toxicity in MH-S cells and Ana-1 cells. We speculated that ZnO particles may have similar toxicity in the normal mouse macrophages, and the toxic effect of dissolved zinc ions may exist a threshold on mouse macrophages.

Compared with the work done by Brunner et al. [4], exposure of MSTO or 3T3 cells to ZnO nanoparticle was characterized by the more steep response pattern, at the concentrations above 15 ppm for 3 days, all MSTO or 3T3 cells died. This may be because some cell debris and cytosol remainders can probably strongly bind Zn^{2+} or ZnO nanoparticles, absorb some of the local Zn^{2+} or ZnO nanoparticles and reduce stress. Limbach et al. studied the uptake kinetics of cerium oxide nanoparticles into human lung fibroblasts at low concentrations [14]. Their results showed that 20–50 nm ceria uptake was a diffusion-limited transport process, but the sedimentation of particles onto the cell was the dominant transport process for 250–400 nm ceria particles at low concentrations. Due to the solubility of ZnO nanoparticles, their uptake kinetics into cell and process of damage cells may be more complex than cerium oxide. Further research is needed. In addition, when the concentration of ZnO particles exceeded 40 μg/ml, the very little decrease in cell viability was observed. This is most probably because the solubility of ZnO particles reached stability.

LDH leakage reflected the cell membrane damage and the degree of cell necrosis. Some studies showed that ZnO nanoparticles could induce LDH leakage in many types of cells, such as mouse neuroblastoma (Neuro-2A) [1], primary mouse embryo fibroblasts (PMEF) [15], human lung epithelial cells (A549) [7], human bronchial epithelial cells (BEAS-2B) [16] and rat alveolar epithelial cell monolayers (RAECMs) [8]. The present study showed that ZnO nanoparticles suspensions and their supernatants led to the significant increase of LDH levels at the concentration of 20 μg/ml and above ($p < 0.05$). ZnO nanoparticles suspensions had more

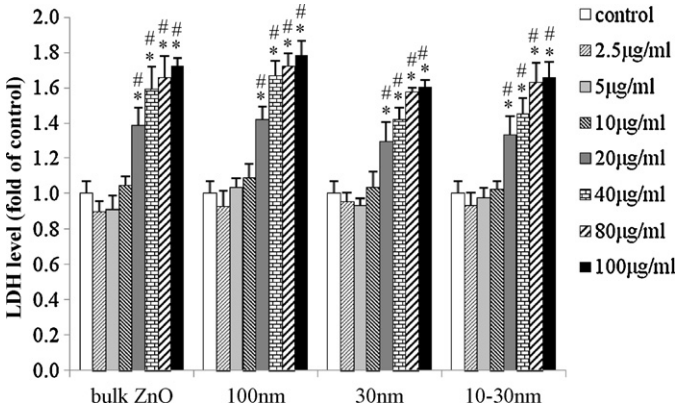

Fig. 3. LDH level in the MH-S cell culture medium following a 24 h exposure to ZnO nanoparticles. Each treatment was conducted five times independently. * $p < 0.05$ vs. control cells, # $p < 0.05$ vs. the corresponding supernatant.

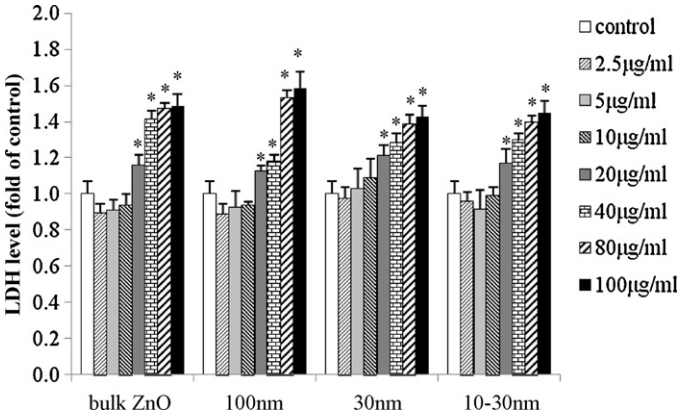

Fig. 4. LDH level in MH-S cell culture medium following a 24 h exposure to supernatant of ZnO nanoparticles suspensions. Each treatment was conducted five times independently. * $p < 0.05$ vs. control cells.

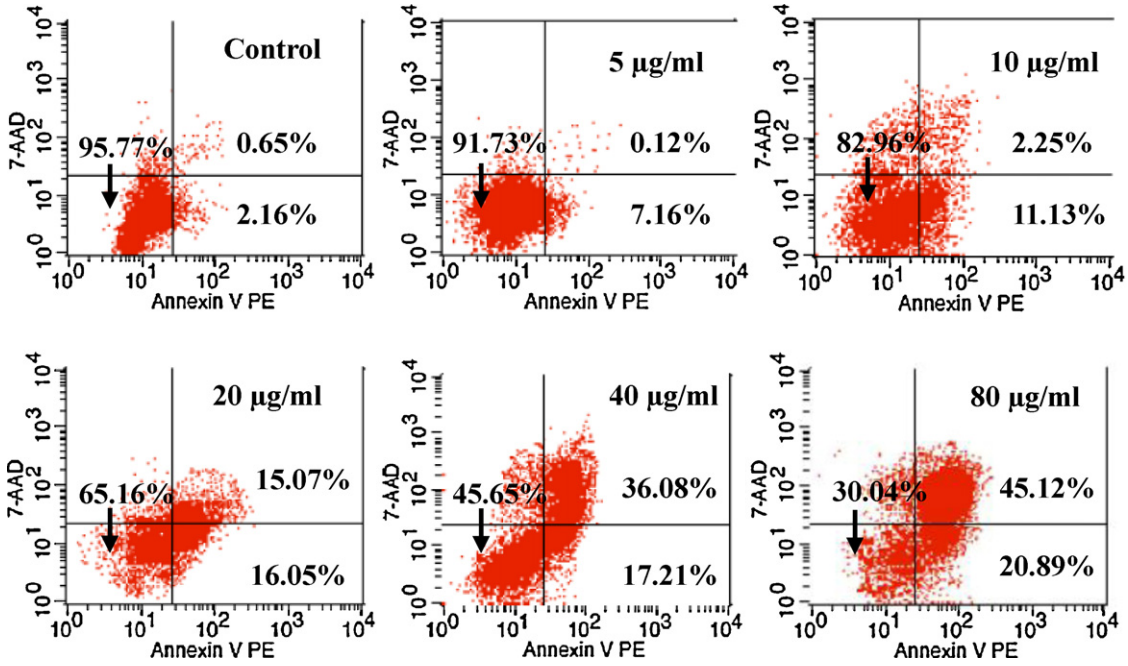

Fig. 5. Flow cytometric analysis of apoptotic cell death after treatments with bulk ZnO particles for 24 h and double labeling with Annexin PE and 7-ADD.

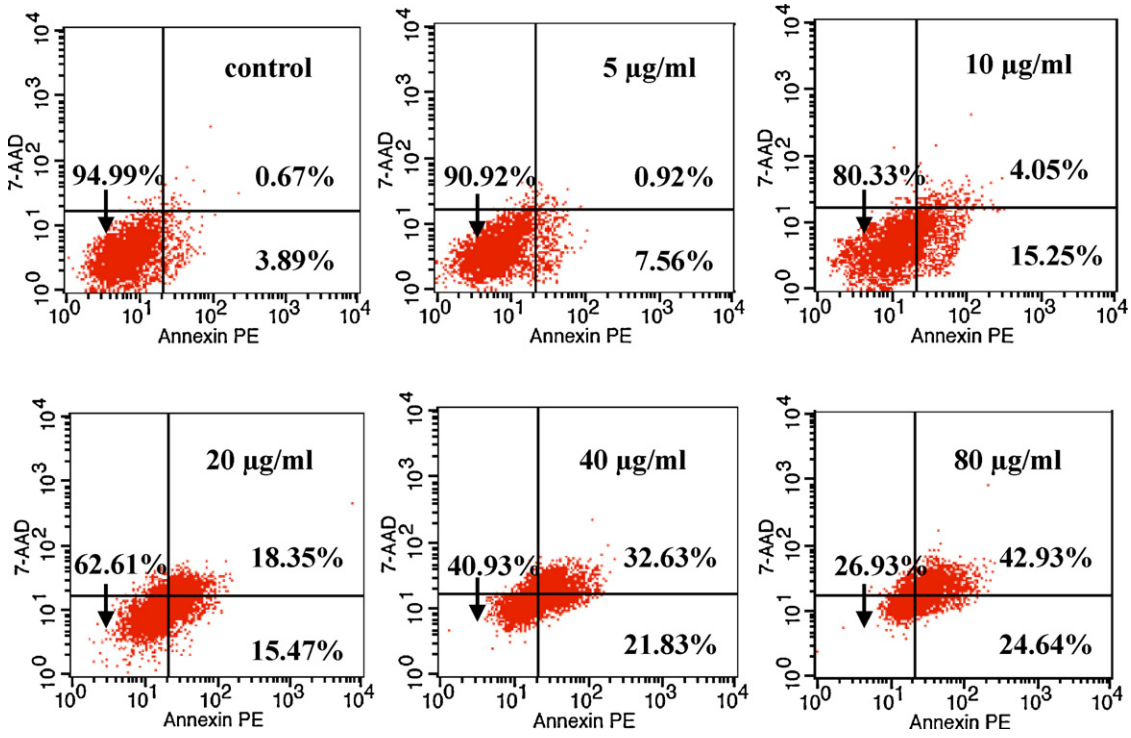

Fig. 6. Flow cytometric analysis of apoptotic cell death after treatments with 100 nm ZnO particles for 24 h and double labeling with Annexin PE and 7-ADD.

pronounced effects than the corresponding supernatants ($p < 0.05$) (Figs. 3 and 4). The results indicated that four ZnO nanoparticles started to induce the cell membrane damage or cell necrosis at the dose of 20 μg/ml and above, dissolved zinc ions played an important role in LDH leakage, besides dissolved zinc ions in cell medium, ZnO particles uptake into cells still could dissolve and release zinc ions. Nondissolved ZnO particles promoted the cell membrane damage. Flow cytometric analysis demonstrated that ZnO particles mainly induced cell apoptosis at dose 5 or 10 μg/ml, and led to cell necrosis at the dose of 20 μg/ml and above (Figs. 5–9).

3.2. Mitochondrial injury and cell apoptosis

Mitochondria are the main cellular sites of ROS production. Intracellular ROS levels were significantly increased after exposure to all ZnO nanoparticles at the dose above 10 μg/ml ($p < 0.05$) (Fig. 10). 10–30 nm ZnO nanoparticles appeared to be more effective. Intracellular ROS levels increased obviously at the dose of 5 μg/ml ($p < 0.05$), and when the dosage was above 20 μg/ml, 10–30 nm ZnO particles produced more intracellular ROS levels than the other ZnO nanoparticles ($p < 0.05$). ROS signaling system

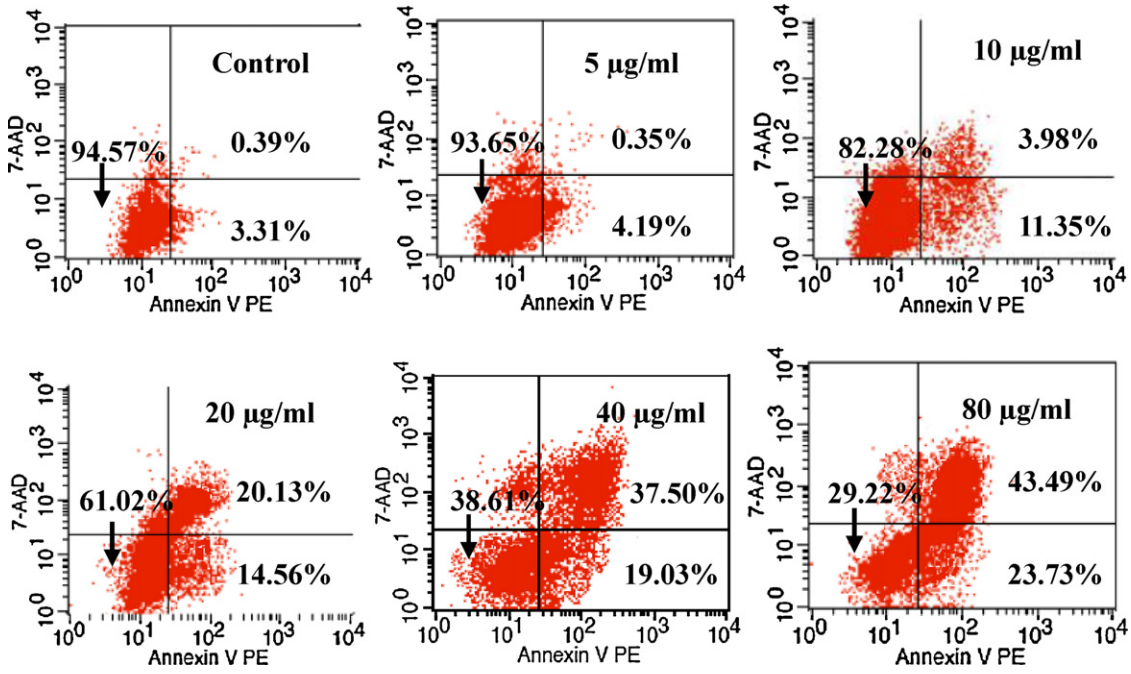

Fig. 7. Flow cytometric analysis of apoptotic cell death after treatments with bulk 5, 10, 20, 40 and 80 μg/ml of 30 nm ZnO particles for 24 h and double labeling with Annexin PE and 7-ADD.

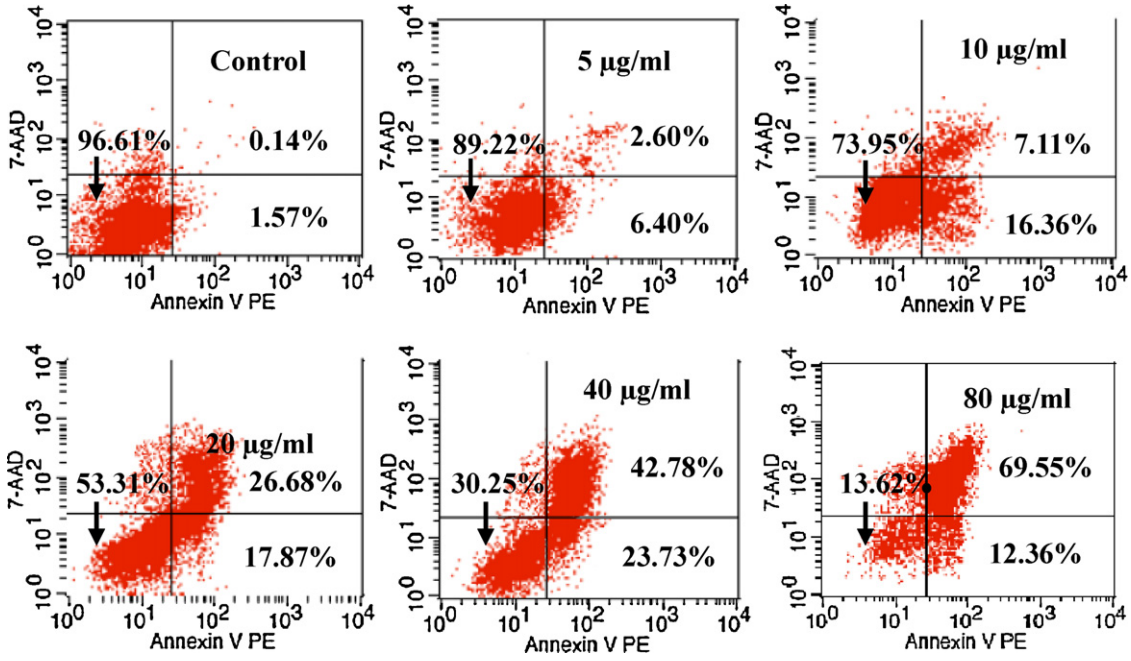

Fig. 8. Flow cytometric analysis of apoptotic cell after treatments with bulk 5, 10, 20, 40 and 80 μg/ml of 10–30 nm ZnO particles for 24 h and double labeling with Annexin PE and 7-ADD.

has a close interaction with the calcium signaling system. ZnO particles exposure induced the obvious increase of intracellular calcium levels (Fig. 11). The rule of intracellular calcium levels was similar with intracellular ROS. The correlation analysis revealed there was a positive correlation between intracellular ROS levels and intracellular calcium levels. The correlation coefficients were 0.889 (bulk ZnO), 0.918 (100 nm), 0.924 (30 nm) and 0.964 (10–30 nm), respectively. The alteration of intracellular calcium levels is related to $\Delta\psi m$. The $\Delta\psi m$ obviously reduced after 24 h of ZnO nanoparticles exposure at the dose above 10 μg/ml ($p < 0.05$) (Fig. 12). When the dosage exceeded 20 μg/ml, the $\Delta\psi m$ of 10–30 nm ZnO nanoparticles treatments were lower than the other ZnO nanoparticles treatments ($p < 0.05$). There was a negative correlation between intracellular ROS levels and the $\Delta\psi m$. The correlation coefficients were −0.980 (bulk ZnO), −0.973 (100 nm), −0.981 (30 nm) and −0.982 (10–30 nm),

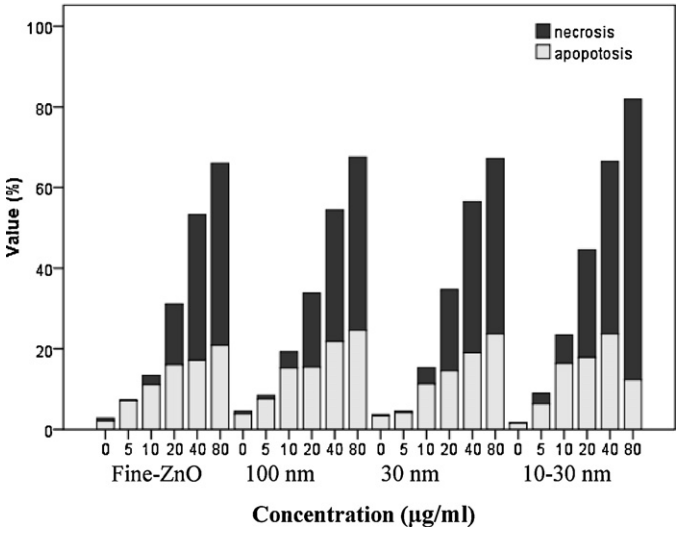

Fig. 9. Apoptotic and necrotic cells after exposure to different sized and concentrations ZnO particles for 24 h.

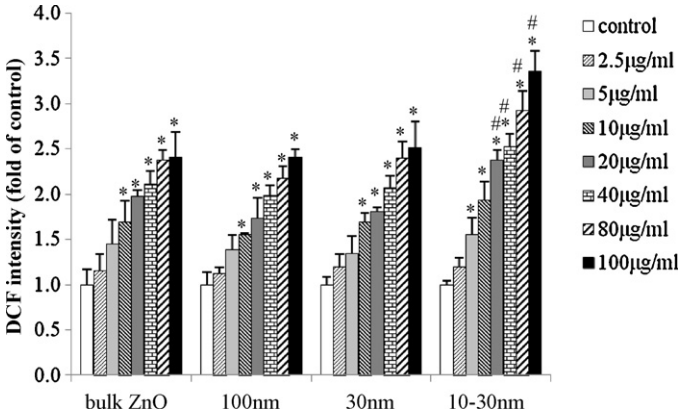

Fig. 10. Oxidative stress induced by exposure of MH-S cells to ZnO nanoparticles. Each treatment was conducted five times independently. * $p < 0.05$ vs. control cells; # $p < 0.05$ vs. other sized ZnO nanoparticles.

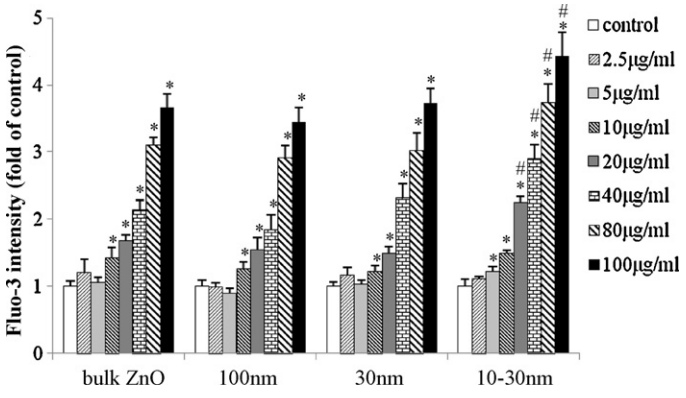

Fig. 11. Intracellular calcium after exposure of MH-S cells to ZnO nanoparticles. Each treatment was conducted five times independently. * $p < 0.05$ vs. control cells; # $p < 0.05$ vs. other sized ZnO nanoparticles.

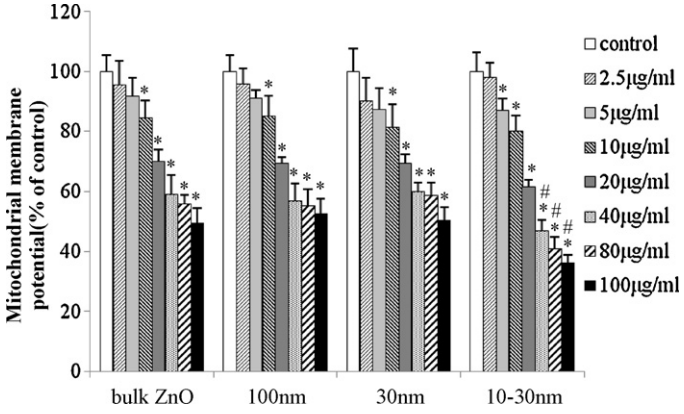

Fig. 12. Mitochondrial membrane potential after exposure of MH-S cells to ZnO nanoparticles. Each treatment was conducted five times independently. * $p < 0.05$ vs. control cells; # $p < 0.05$ vs. other sized ZnO nanoparticles.

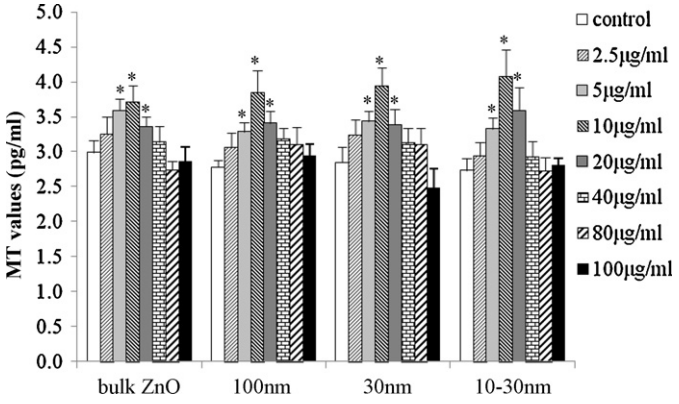

Fig. 13. MT protein levels in MH-S after 24 h of ZnO nanoparticles exposure. Each treatment was conducted three times independently. * $p < 0.05$ vs. control cells.

respectively. The increase of intracellular calcium and the decrease of $\Delta\psi m$ destroyed mitochondrial function and led to cell apoptosis. The results of cell apoptosis showed that the numbers of apoptotic and necrosis cells increased markedly at the dose above 10 μg/ml (Fig. 9). 10–30 nm ZnO particles induced more apoptotic and necrosis cells than other three ZnO particles.

It has been demonstrated that nanomaterials of various sizes and chemical compositions preferentially mobilized to mitochondria and destroyed mitochondrial function [17–19]. Mitochondria also were target organelles for cytotoxic injury of zinc ions [20–22]. Berardis et al. showed that ZnO nanoparticles induced significant oxidative stress and mitochondrial disfunction, probably due to a direct interaction of ZnO nanoparticles with some components of the cell surface [23]. Huang et al. found that ZnO nanoparticles induced the increase of intracellular calcium levels in BEAS-2B cells [16]. The author suggested that ZnO particles might first interact with cytoplasm membrane causing loss of membrane integrity leading to calcium influx through membrane channels. In this study, ZnO particles led to the increase of intracellular calcium at the concentration 10 μg/ml or 5 μg/ml, but did not induce LDH leakage. It indicated that this increase might mainly derive from intracellular calcium store release, not from the influx of extracellular calcium. Meanwhile, ZnO particles induced the obvious decrease of $\Delta\psi m$ at the concentration 10 μg/ml or 5 μg/ml. These results indicated that dissolved zinc ions easily entered into cells, reached mitochondria, and altered mitochondrial functionality. Therefore, the effect of dissolved zinc ions was faster than ZnO particles. After dissolved zinc ions led to cell damage, ZnO particles more easily entered into cell, caused toxicity. When the concentration exceeded 40 μg/ml, the toxic effect of dissolved zinc ions in cell medium reached the threshold. 10–30 nm ZnO particles induced more apoptotic and necrosis cells, probably mainly due to the role of nondissolved ZnO particles. Apart from interaction with the cell membrane, particle characteristics may be effect the particle uptake. Thus the internalized amount of different ZnO particles may be different. Intracellular dissolved zinc still exist difference. In addition, the effect of intracellular nondissolved ZnO particles on cells may be also different. Particles shape and surface area may affect their toxicity. The toxic effect of rod ZnO particles was able to lower than spherical ZnO particles. Nair et al. also found that rod ZnO nanoparticles were lower toxic than spherical ZnO nanoparticles. Moreover, surface area of 10–30 nm ZnO particles was significantly larger than the other three ZnO particles [24]. Hsiao and Huang found that regardless of their shape, ZnO nanoparticles having larger SSAs might provoke more serious toxicity on A549 cells [25]. In addition, toxic effect of ZnO nanoparticles still may depend on the structural and electronic characteristics of particles surface, which needs to be explored in further study.

3.3. Oxidation and antioxidation of zinc

A small amount of zinc ions served as an effective antioxidant. MT is a protein with the most effective scavenging free radical, and plays an important role in antioxidant of zinc. A number of in vitro and in vivo studies have shown that induction of MT synthesis by Zn played a protective role in cellular response to oxidative stress [10,26–34]. Alscher et al. found that the antioxidative effect of MT was equal to NAC and glutathione [28]. At present, the mechanism by which MT scavenges the radicals is not entirely clear. MT might function as an expendable target for oxidant due to its highly enriched cysteine residue structure. Oxidative conditions resulted in oxidation of MT thiolate groups and release of Zn [29,33,34].

The exposure of cells in culture to moderate concentrations of Zn ions is a well-known way to generate up-regulation of MTs [10,35]. Alscher et al. showed that zinc (5–15 μg/ml Zn) caused a dose-dependent increase of MT in Epithelial tubular cells derived from swine kidney (LLC-PK1 cells). Baird et al. found that exposure to 100 μM Zn (in the form of ZnSO4) for 12–24 h significantly and time-dependently increased cellular MT [10]. In this study, MT assay showed that when the concentration of ZnO nanoparticles was 5–20 μg/ml, MT contents in MH-S cells were significantly increased ($p < 0.05$), and reached the highest level at the dose of 10 μg/ml. MT contents started to decrease at the dose above 20 μg/ml (Fig. 13). The results indicated that oxidation resistance of dissolved zinc ions reached the strongest level at the dose of 10 μg/ml. When the concentration of ZnO particles exceeded 20 μg/ml, cell damage was more serious, unable to synthesize enough MT to bind excessive zinc, oxidation resistance started to reduce. Excessive zinc induced mitochondrial damage, generated more intracellular ROS, and further destroyed cell structure. The results of LDH and cell apoptosis also demonstrated that 5 or 10 μg/ml ZnO particles had lower toxicity. At the dose above 20 μg/ml, the toxicity of ZnO particles increased steeply. Intracellular ROS still increased at the dose below 20 μg/ml, it might be partly due to taking time for MT synthesis. Thus MT could partly reduce oxidative stress induced by ZnO nanoparticles, but not completely resist it.

4. Conclusion

ZnO particles had similar toxicity in MH-S cells and Ana-1 cells. At the concentration of ZnO particles less than or equal to 10 μg/ml, dissolved zinc ions induced metallothionein synthesis to reduce oxidative damage, ZnO particles mainly induced cell apoptosis.

When the concentration of ZnO particles exceeded 20 μg/ml, excessive zinc destroyed mitochondrial function and cell membrane, caused cell necrosis. The toxicity of dissolved zinc ions existed a threshold. The toxic difference of different ZnO particles mainly depended on the role of nondissolved ZnO particles.

Conflict of interest statement

None declared.

Acknowledgment

The authors are grateful to the financial support from the National Natural Science Foundation of China (30771771, 21007045, 30800934 and 30901221) and the Natural Science Foudation of Tianjin (10JCZDJC17100).

References

[1] H.A. Jeng, J. Swanson, Toxicity of metal oxide nanoparticles in mammalian cells, J. Environ. Sci. Health Part A: Toxic/Hazard. Subst. Environ. Eng. 41 (2006) 2699–2711.
[2] J.C.K. Lai, M.B. Lai, S. Jandhyam, V.V. Dukhande, A. Bhushan, C.K. Daniels, S.W. Leung, Exposure to titanium dioxide and other metallic oxide nanoparticles induces cytotoxicity on human neural cells and fibroblasts, Int. J. Nanomed. 3 (2008) 533–545.
[3] M. Horie, K. Nishio, K. Fujita, S. Endoh, A. Miyauchi, Y. Saito, H. Iwahashi, K. Yamamoto, H. Murayama, H. Nakano, N. Nanashima, E. Niki, Y. Yoshida, Protein adsorption of ultrafine metal oxide and its influence on cytotoxicity toward cultured cells, Chem. Res. Toxicol. 22 (2009) 543–553.
[4] T.J. Brunner, P. Wick, P. Manser, P. Spohn, P.N. Grass, L. Limbach, A. Bruinink, W.J. Stark, In vitro cytotoxicity of oxide nanoparticles: comparison to asbestos, silica, and the effect of particle solubility, Environ. Sci. Technol. 40 (2006) 4374–4381.
[5] H.L. Karlsson, P. Cronholm, J. Gustafsson, L. Möller, Copper oxide nanoparticles are highly toxic: a comparison between metal oxide nanoparticles and carbon nanotubes, Chem. Res. Toxicol. 21 (2008) 1726–1732.
[6] T. Xia, M. Kovochich, M. Liong, L. Ma dler, B. Gilbert, H. Shi, J.I. Yeh, J.I. Zink, A.E. Nel, Comparison of the mechanism of toxicity of zinc oxide and cerium oxide nanoparticles based on dissolution and oxidative stress properties, ACS Nano 2 (2008) 2121–2134.
[7] W. Lin, Y. Xu, C.C. Huang, Y. Ma, K.B. Shannon, D.R. Chen, Y.W. Huang, Toxicity of nano- and micro-sized ZnO particles in human lung epithelial cells, J. Nanopart. Res. 11 (2009) 25–39.
[8] Y.H. Kim, F. Fazlollahi, I.M. Kennedy, N.R. Yacobi, S.F. Hamm-Alvarez, Z. Borok, K.J. Kim, E.D. Crandall, Alveolar epithelial cell injury due to zinc oxide nanoparticle exposure, Am. J. Respir. Crit. Care Med. 182 (2010) 1398–1409.
[9] W. Song, J. Zhang, J. Guo, J. Zhang, F. Ding, L. Li, Z. Sun, Role of the dissolved zinc ion and reactive oxygen species in cytotoxicity of ZnO nanoparticles, Toxicol. Lett. 199 (2010) 389–397.
[10] S.K. Baird, T. Kurz, U.T. Brunk, Metallothionein protects against oxidative stress-induced lysosomal destabilization, Biochem. J. 394 (2006) 275–283.
[11] L.A. Morio, K.A. Hooper, J. Brittingham, T.H. Li, R.E. Gordon, B.J. Turpin, D.L. Laskin, Tissue injury following inhalation of fine particulate matter and hydrogen peroxide is associated with altered production of inflammatory mediators and antioxidants by alveolar macrophages, Toxicol. Appl. Pharm. 177 (2001) 188–199.
[12] A. Beyerle, S. Holger, T. Kissel, T. Stoeger, Screening strategy to avoid toxicological hazards of inhaled nanoparticles for drug delivery: the use of α-quartz and nano zinc oxide particles as benchmark, J. Phys.: Conf. Ser. 151 (2009) 012034.
[13] C.P. Wan, E. Myung, B.H. Lau, An automated micro-fluorometric assay for monitoring oxidative burst activity of phagocytes, J. Immunol. Methods 159 (1993) 131–138.
[14] L.K. Limbach, Y. Li, R.N. Grass, T.J. Brunner, M.A. Hintermann, M. Muller, D. Gunther, W.J. Stark, Oxide nanoparticle uptake in human lung fibroblasts: effects of particle size, agglomeration, and diffusion at low concentrations, Environ. Sci. Technol. 39 (2005) 9370–9376.
[15] H. Yang, C. Liu, D. Yang, H. Zhang, Z. Xi, Comparative study of cytotoxicity, oxidative stress and genotoxicity induced by four typical nanomaterials: the role of particle size, shape and composition, J. Appl. Toxicol. 29 (2009) 69–78.
[16] C.C. Huang, R.S. Aronstam, D.R. Chen, Y.W. Huang, Oxidative stress, calcium homeostasis, and altered gene expression in human lung epithelial cells exposed to ZnO nanoparticles, Toxicol. In Vitro 24 (2010) 45–55.
[17] S. Foley, C. Crowley, M. Smaihi, C. Bonfils, F.B. Erlanger, P. Seta, C. Larroque, Cellular localization of a water-soluble fullerene derivatives, Biochem. Biophys. Res. Commun. 294 (2002) 116–119.
[18] N. Li, C. Sioutas, A. Cho, D. Schmitz, C. Misra, J. Sempf, M. Wang, T. Oberley, J. Froines, A. Nel, Ultrafine particulate pollutants induce oxidative stress and mitochondrial damage, Environ. Health Perspect. 111 (2003) 455–460.
[19] R. Savic, L. Luo, A. Eisenberg, D. Maysinger, Micellar nanocontainers distribute to defined cytoplasmic organelles, Science 300 (2003) 615–618.
[20] D.A. Wiseman, S.M. Wells, M. Hubbard, J.E. Welker, S.M. Black, Alterations in zinc homeostasis underlie endothelial cell death induced by oxidative stress from acute exposure to hydrogen peroxide, Am. J. Physiol. Lung Cell. Mol. Physiol. 292 (2007) L165–L177.
[21] P. Marin, M. Israel, J. Glowinske, J. Premont, Routes of zinc entry in mouse cortical neurons: role in zinc-induced neurotoxicity, Eur. J. Neurosci. 12 (2000) 8–18.
[22] W.M.U. Daniels, J. Hendricks, R. Salie, S.J. van Rensburg, Amechanism for zinc toxicity in neuroblastoma cells, Metab. Brain Dis. 19 (2004) 79–88.
[23] B.D. Berardis, G. Civitelli, M. Condello, P. Lista, R. Pozzi, G. Arancia, S. Meschini, Exposure to ZnO nanoparticles induces oxidative stress and cytotoxicity in human colon carcinoma cells, Toxicol. Appl. Pharmacol. 246 (2010) 116–127.
[24] S. Nair, A. Sasidharan, V.V. Divya Rani, D. Menon, S. Nair, K. Manzoor, S. Raina, Role of size scale of ZnO nanoparticles and microparticles on toxicity toward bacteria and osteoblast cancer cells, J. Mater Sci.: Mater Med. 20 (2009) S235–S241.
[25] I.L. Hsiao, Y.J. Huang, Effects of various physicochemical characteristics on the toxicities of ZnO and TiO_2 nanoparticles toward human lung epithelial cells, Sci. Total Environ. 409 (2011) 1219–1228.
[26] R. Sharma, M. Sharma, P.K. Datta, V.J. Savin, Induction of metallothionein-I protects glomeruli from superoxide-mediated increase in albumin permeability, Exp. Biol. Med. 227 (2002) 26–31.
[27] X. Li, H. Chen, P.N. Epstein, Metallothionein protects islets from hypoxia and extends islet graft survival by scavenging most kinds of reactive oxygen species, J. Biol. Chem. 279 (2004) 765–771.
[28] D.M. Alscher, N. Braun, D. Biegger, C. Stuelten, K. Gawronski, T.E. Mürdter, U. Kuhlmann, P. Fritz, Induction of metallothionein in proximal tubular cells by zinc and its potential as an endogenous antioxidant, Kidney Blood Press. Res. 28 (2005) 127–133.
[29] Z.E. Suntres, E.M.K. Lui, Antioxidant effect of zinc and zinc-metallothionein in the acute cytotoxicity of hydrogen peroxide in Ehrlich ascites tumour cells, Chem. Biol. Interact. 162 (2006) 11–23.
[30] S.R. Davis, R.J. Cousins, Metallothionein expression in animals: a physiological perspective on function, J. Nutr. 130 (2000) 1085–1088.
[31] S.R. Davis, D.A. Samuelson, R.J. Cousins, Metallothionein expression protects against carbon tetrachloride-induced hepatotoxicity, but overexpression and dietary zinc supplementation provide no further protection in metallothionein transgenic and knockout mice, J. Nutr. 131 (2001) 215–222.
[32] V. Medici, A. Santon, G.C. Sturniolo, R. D'Incà, S. Giannetto, V. Albergoni, P. Irato, Metallothionein and antioxidant enzymes in Long-Evans cinnamon rats treated with zinc, Arch. Toxicol. 76 (2002) 509–516.
[33] A. Markant, I. Pallaup, Metallothionein and zinc as potential antioxidants in radical-induced lipid peroxidation in cultured hepatocytes, J. Trace Elem. Med. Biol. 10 (1996) 88–95.
[34] A. Formigari, P. Irato, A. Santon, Zinc, antioxidant systems and metallothionein in metal mediated-apoptosis: biochemical and cytochemical aspects, Comp. Biochem. Physiol.: Part C 146 (2007) 443–459.
[35] G.K. Andrews, Regulation of metallothionein gene expression by oxidative stress and metal ions, Biochem. Pharmacol. 59 (2000) 95–104.